

Pairwise Sequency Index Modulation With OTSM for Green and Robust Single-Carrier Communications

Abed Doosti-Aref¹, Member, IEEE, Christos Masouros², Fellow, IEEE, Ertugrul Basar³, Fellow, IEEE, and Huseyin Arslan⁴, Fellow, IEEE

Abstract—In this letter, inspired by the fundamental thoughts of sequency index modulation (SeIM) and orthogonal time sequency multiplexing (OTSM), a novel technique is introduced for green and robust single-carrier communications in wireless networks. More specifically, pairwise SeIM (PSeIM) is proposed as a novel indexing scheme making SeIM robust to error propagation and significantly reduces the peak power of SeIM-based systems with a lower complexity of detection. Analytical results are presented for the bit error rate (BER), peak-to-average power ratio (PAPR), and spectral efficiency to reveal the trade-off and advantages in PSeIM-OTSM. Simulation and analytical results verify that for 4-QAM uncoded data, PSeIM-OTSM outperforms OTSM by 50% in terms of both PAPR and complexity of detection along with 125.32% energy efficiency improvement to achieve a BER of 10^{-8} in high mobility doubly spread channels.

Index Terms—OTSM, sequency index modulation, green communications, vehicular communications.

I. INTRODUCTION

IN THE sixth generation (6G) of wireless networks, employing millimeter-wave and beyond frequency bands, single-carrier (SC) waveforms confront fewer challenges rather than multi-carrier (MC) ones in high mobility doubly spread channels (DSCs) [1]. Index modulation (IM) is a flexible technique improving the system performance in terms of bit error rate (BER) and energy efficiency (EE) with a low implementation complexity [2], [3]. Thus, combining an SC waveform, performing as good as MC waveform in DSCs, with an appropriate IM scheme, can meet the robust and green communication demands more efficiently than MC systems in Internet of things and vehicle-to-vehicle communications [1], [2], [3].

Orthogonal time sequency multiplexing (OTSM) has been recently proposed as a promising SC waveform in the delay-sequency (DS) domain, offering comparable BER to

MC orthogonal time frequency space modulation in high mobility DSCs. However, it is significantly less complex due to the low implementation complexity of Walsh-Hadamard transform (WHT) [4], [5]. Thanks to the WHT, the modulation and demodulation in OTSM are implemented only through addition/subtraction making it less complex than conventional SC waveforms such as SC orthogonal frequency division multiplexing (SC-OFDM) and other fast Fourier transform based waveforms [4], [5], [6], [7]. Furthermore, in SC-OFDM and other time-frequency (TF) domain waveforms, since the signal is one-dimensional (1D), the DSC impairments such as delay and Doppler are not resolvable in TF domain whereas they are separable in OTSM being a 2D signal, giving rise to a nearly constant signal-to-noise ratio (SNR) in the DS domain [4], [5]. Such properties along with the low-complexity detection and signal processing in the DS domain [8] have made OTSM a suitable candidate for green SC communications in the 6G wireless networks. In [3], instead of using channel coding, sequency index modulation (SeIM) is suggested as a potential IM scheme for DS domain waveforms like OTSM to boost the BER and EE. The SeIM technique utilizes the sequency as an index to apply IM through activating and deactivating sequency bins to convey extra signaling. It employs on-off keying (OOK) as a method of information transmission to implement IM. However, error propagation extremely affects SeIM decoding since incorrectly detected activated sequencies in low SNR values will result in errors in the demodulation of symbols that are encoded over those sequency bins.

In this letter, we propose a new sequency indexing approach referred to as pairwise SeIM (PSeIM) to address the SeIM issues for robustness and energy efficiency in SeIM based communication systems. In PSeIM by encoding information over pairs of sequencies, error propagation is prevented and the need to apply OOK threshold is removed. As a result, the BER is drastically reduced with a lower complexity of detection. The lowering of the peak-to-average power ratio (PAPR) is another advantage of PSeIM. In addition, building on the promising combination of PSeIM and OTSM, we propose PSeIM-OTSM as a new technique, outperforming both OTSM and SeIM-OTSM [3] in terms of BER, EE, and PAPR with a lower implementation complexity. These novel ideas have been inspired by a desire to increase the reliability with low latency and minimize energy consumption being essential in the 6G green vehicular communication networks.

Motivated by the above background, the contributions in this letter are summarized as follows.

- i) PSeIM is proposed as a new IM scheme in the DS domain.
- ii) PSeIM-OTSM is proposed for green SC communications, offering higher EE with lower BER, PAPR, and complexity of detection compared to both SeIM-OTSM [3] and OTSM.

Manuscript received 21 December 2023; accepted 26 January 2024. Date of publication 30 January 2024; date of current version 11 April 2024. The work of Ertugrul Basar was supported by TUBITAK under Grant 121C254. The associate editor coordinating the review of this article and approving it for publication was Y. Mao. (Corresponding author: Abed Doosti-Aref.)

Abed Doosti-Aref is with the School of Electrical Engineering, Sharif University of Technology, Tehran 11155-1639, Iran (e-mail: a.doosti@sharif.edu).

Christos Masouros is with the Department of Electronic and Electrical Engineering, University College London, WC1E 6BT London, U.K. (e-mail: c.masouros@ucl.ac.uk).

Ertugrul Basar is with the College of Engineering, Department of Electrical and Electronics Engineering, Koc University, 34450 Istanbul, Turkey (e-mail: ebasar@ku.edu.tr).

Huseyin Arslan is with the School of Engineering and Natural Sciences, Istanbul Medipol University, 34810 Istanbul, Turkey (e-mail: huseyinarslan@medipol.edu.tr).

Digital Object Identifier 10.1109/LWC.2024.3360256

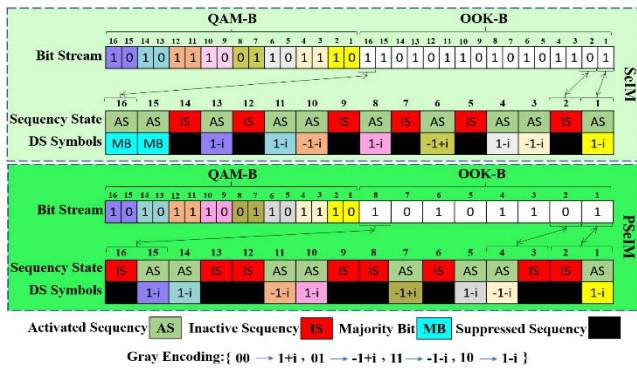


Fig. 1. Proposed PSeIM compared to classical SeIM for 4-QAM and $N=16$.

iii) A closed-form expression is analytically derived for the BER of PSeIM-OTSM in the presence of additive white gaussian noise (AWGN) and Rayleigh fading.

iv) Analytical results are derived for the PAPR and spectral efficiency (SE) of PSeIM-OTSM to be compared with both SeIM-OTSM [3] and OTSM.

The rest of this letter is organized as follows. Section II describes the proposed PSeIM scheme. The PSeIM-OTSM signaling along with the analytical expressions for BER, PAPR, and SE are presented in Section III followed by the performance evaluations discussed in Section IV. Finally, conclusions are summarized in Section V.

II. PROPOSED PAIRWISE SEQUENCY INDEX MODULATION

A. SeIM and Its Limitations in Green Communications

In SeIM, each input bitstream has a length of $\frac{N \log_2 Q}{2} + N$ where N is the number of sequency bins and Q is the size of the Q -ary quadrature amplitude modulation (QAM). The input bitstream is split into two sub-bitstreams. The sub-bitstream formed by the N initial bits, shown in Fig. 1 as OOK-B, is utilized to find the majority bit (MB) type through the calculation of Hamming weight of OOK-B. The type of MB is 1 if the Hamming weight becomes equal or larger than $\frac{N}{2}$; otherwise, it is 0. The number of bits in OOK-B with the MB type is denoted by μ_{MB} [3]. If the type of a bit in OOK-B is the same with the type of MB, the related sequency bin is stated as activated sequency (AS); otherwise, it is marked as inactive sequency (IS). The second sub-bitstream, shown in Fig. 1 as QAM-B, is made up of the final $\frac{N \log_2 Q}{2}$ bits. The value of IS bins is considered to be 0 and the complex numbers corresponding to the QAM constellation symbols required to encode QAM-B based on the Gray encoding, will be assigned to the values of the first $\frac{N}{2}$ AS bins. The receiver can be informed of the MB type using the remaining AS bins, and they will be provided a signal having a power equal to the required average power for the specified Q -QAM. At the receiver, all sequency bins are first examined. Those sequency bins whose power exceed a threshold are stated as AS and the rest are marked as IS. Following that, OOK-B is rebuilt by the identified sequency states and MB type. Then, to obtain QAM-B and merge it with OOK-B, the first $\frac{N}{2}$ AS bins are demodulated using the Q -QAM Gray decoding.

The functionality of SeIM is restricted by two key problems in green communications. First, the threshold of OOK detector

should be less powerful than the Q -QAM symbol with the lowest power. This constraint gives rise to a more energy consumption and complexity of detection in the applications employing high QAM orders. Second, in low SNR values, inaccurate sequency state detection causes all ensuing bits in that section of the frame to be misplaced. To cope with such error propagation, forward error correcting codes should be utilized, imposing further latency, complexity, and energy consumption to the transceiver. In what follows, we propose a new sequency indexing scheme to address mentioned issues.

B. Proposed Pairwise Sequency Indexing Scheme

In PSeIM, as depicted in Fig. 1, each bit from OOK-B is encoded as a pair of ‘on-off’ sequencies, as opposed to encoding each bit through a single sequency state in SeIM. Accordingly, whenever a ‘1’ appears in OOK-B, the first sequency of the pair is set as AS and the second is set as IS. Whenever a ‘0’ appears in OOK-B, the first sequency of the pair is stated as IS and the second to be AS. As a result, the amount of OOK-B that can be represented by sequency states is $\frac{N}{2}$, namely half of that in the classical SeIM. The advantage is that one of the sequences in each pair is always activated and the other one is inactive. This therefore removes the need for calculating the MB type at the transmitter and signaling the MB type to the receiver. In addition, it removes thresholding and replaces it with a power comparison between the sequencies of a pair, where the higher is identified as AS and the lower as IS. This further results in a drastic reduction of the error propagation. Moreover, bits from QAM-B can no longer be lost as a consequence of erroneously identifying earlier sequency states. As a result, within each pair, the amount of error that can be made is constrained.

III. PROPOSED PSEIM-OTSM

In this section, building on the promising combination of PSeIM and OTSM, a new signaling methodology is proposed whose transceiver block diagram is shown in Fig. 2.

At the transmitter, frames of length $M(\frac{N \log_2 Q}{2} + \frac{N}{2})$ bits are equally split into M branches as the M input bitstreams of the bit splitter. Each input bitstream of length $\frac{N \log_2 Q}{2} + \frac{N}{2}$ is divided into two bit-substreams of length $\frac{N}{2}$ and $N \log_2 Q / 2$ which are given to OOK-B and QAM-B blocks, respectively, to implement PSeIM encoding based on the method described in Section II. B. Let $\mathbf{X}_e \in \mathbb{C}^{M \times N}$ denote the matrix in DS domain at the output of PSeIM encoder in which $M \times \frac{N}{2}$ AS bins are allocated to Q -QAM complex numbers and $M \times \frac{N}{2}$ IS bins are zero. To implement interleaved zero padding (ZP) among blocks, the last $2l_{max}+1$ rows of \mathbf{X}_e are arranged to zero, where l_{max} denotes the maximum normalized delay shift of the DSC. To move from the DS domain to delay-time (DT) domain, an N -point inverse WHT (IWHT) is applied along the sequency domain, namely each row of \mathbf{X}_e as $\tilde{\mathbf{X}}_e = \mathbf{X}_e \mathbf{W}_N$ where \mathbf{W}_N denotes the unitary N -square WHT/IWHT matrix. The DT samples are then column-wise vectorized to generate the time domain samples vector $\tilde{\mathbf{S}}_e \in \mathbb{C}^{MN \times 1} = \text{vec}(\tilde{\mathbf{X}}_e)$. A cyclic prefix (CP) of length l_{max} is copied from the end of the time domain vector and it is appended as a preamble at the head of the time domain vector.

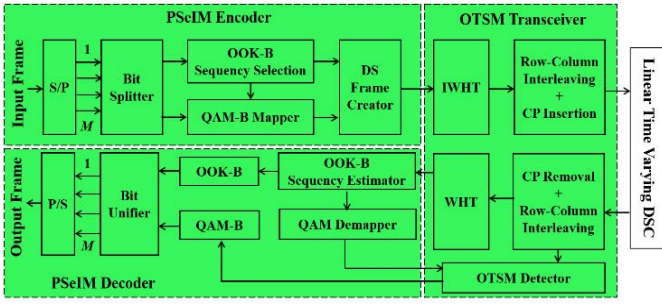


Fig. 2. Schematic block diagram of Proposed PSeIM-OTSM.

The samples are then pulse shaped through a rectangular pulse $p(t)$ having a duration of T to be transmitted as

$$s_e(t) = \sum_{m=0}^{M-1} \sum_{n=0}^{N-1} \tilde{s}_e[m + nM]p(t - nT), \quad (1)$$

where $\tilde{s}_e[m + nM] = \sum_{i=0}^{N-1} \mathbf{X}_e[m, i] \mathbf{W}_N[i, n]$.

At the receiver, after removing the CP, the time domain channel impaired vector is folded back to represent the DT matrix. Then, N -point WHT is applied over each row of the DT matrix to obtain the DS representation of the received symbols as the input of the PSeIM decoder. Then, bits of the OOK-B are detected through the detected sequency pairs, which are identified by the power comparison described in Section II-B. Having the indices of the activated sequencies over each delay bin, the OTSM detector is then utilized to decode the information bits of the received QAM symbols. Finally, the detected OOK-B is merged with the detected QAM-B through the bit unifier as the detected bitstream B.

A. The BER Analysis

To calculate BER, we assume each sequency pair in the received bitstream undergoes Rayleigh fading in the presence of AWGN. We define P_{TF} as the transmit power allocated to each DS frame, ρ as the fading amplitude, and σ^2 as the AWGN power per sequency. Let $P_e(E_B)$, $P_e(E_{OOK-B})$, and $P_e(E_{QAM-B})$ denote the error probability for estimation process of bitstream B, OOK-B, and QAM-B, respectively. Since the length of OOK-B and QAM-B are $\frac{N}{2}$ and $N \log_2^Q / 2$, respectively, $P_e(E_B)$ can be written as

$$P_e(E_B) = \left(\frac{1}{1 + \log_2^Q} \right) P_e(E_{OOK-B}) + \left(\frac{\log_2^Q}{1 + \log_2^Q} \right) \times P_e(E_{QAM-B}). \quad (2)$$

To calculate $P_e(E_{OOK-B})$ we know that in the presence of fading, when the Gaussian distribution is centered at the origin of QAM constellation and the distance between the QAM symbol and the origin is d , the probability that the AS and IS of a pair are erroneously distinguished for a given AS bin power of d^2 , utilized to convey QAM symbol, is obtained by $Q\left(\frac{\rho d}{\sigma}\right)$ where $Q(\cdot)$ denotes the Gaussian tail distribution function [9]. In addition, the value of the AS bin before the addition of AWGN and experiencing fading may have been equal to any one of the Q constellation points with an equal chance of $1/Q$. Hence, the probability that the power of AS bin is equal to the power of each constellation point namely d_i^2 is expressed

as a weighted sum of Q different probability densities coming from the Gaussian distributions centered at the Q constellation points [9]. Therefore, based on the conditional probability law and total probability theorem, the probability that AS and IS are incorrectly determined in a sequency pair can be written as

$$P_e(E_{OOK-B}) = \frac{1}{Q} \sum_{i=1}^Q \int_0^\infty Q\left(\frac{\rho d_i}{\sigma}\right) f_\rho(\rho) d\rho, \quad (3)$$

where $f_\rho(\rho)$ denotes the probability density function of Rayleigh distribution [9]. Accordingly, the complementary probability that the AS and IS are correctly identified in a sequency pair is written as $\bar{P}_e(E_{OOK-B}) = 1 - P_e(E_{OOK-B})$.

When a sequency state is incorrectly detected, an attempt is still made to demodulate an unmodulated sequency using Q -QAM, which introduces further errors into the frame. Also, symbols encode bits which differ by only one bit on average when the Q -QAM constellation is Gray encoded. Thus, in most of the cases, only one bit will be in error with the probability of $\frac{(\log_2^Q - 1)}{\log_2^Q}$ due to the erroneously detection of OOK-B. Hence, the first part of the BER contribution of QAM-B is equal to $\frac{P_e(E_{OOK-B})(\log_2^Q - 1)}{\log_2^Q}$. In addition, when a sequency state is correctly detected, the contribution of QAM-B to the overall BER can be considered as P_e^{Q-QAM} namely the BER of Q -QAM in the presence of AWGN and fading given in [9]. Thus $P_e(E_{QAM-B})$ is written as

$$P_e(E_{QAM-B}) = P_e(E_{OOK-B}) \frac{(\log_2^Q - 1)}{\log_2^Q} + \bar{P}_e(E_{OOK-B}) P_e^{Q-QAM}, \quad (4)$$

where $P_e^{Q-QAM} = 2\alpha(1 - \lambda - \alpha/2 + (\alpha\lambda \tan^{-1}(1/\lambda))/2\pi)$, $\alpha = \frac{(\sqrt{Q}-1)}{\sqrt{Q}}$, and $\lambda = \rho \sqrt{\frac{3P_{TF}}{(MN\sigma^2(Q-1) + 3\rho^2 P_{TF})}}$.

B. The PAPR Analysis

To calculate PAPR, we first sample from (1) with a period of T_s to obtain the discrete-time representation of (1) as

$$s_e(qT_s) = \sum_{m=0}^{M-1} \sum_{n=0}^{N-1} \sum_{i=0}^{N-1} \mathbf{X}_e[m, i] \mathbf{W}_N[i, n] p(qT_s - nT), \quad (5)$$

where $q = 0, 1, \dots, NM - 1$. Accordingly, PAPR is defined as

$$\text{PAPR} = \frac{\max(|s_e(qT_s)|^2)}{\frac{1}{MN} \sum_{q=0}^{NM-1} |s_e(qT_s)|^2}. \quad (6)$$

Samples of $\mathbf{X}_e[m, n]$ correspond to the Q -QAM mapping of a memoryless information source equiprobably decorated in the DS grid with an equal chance of $\frac{1}{MN}$. Thus $\mathbf{X}_e[m, n]$ can be assumed as a zero-mean random variable with a sample variance of $\sigma_F^2 = \frac{1}{MN} \sum_{m=0}^{M-1} \sum_{n=0}^{N-1} |\mathbf{X}_e[m, n]|^2$, which is also equal to the average power of the Q -QAM constellation. Using Cauchy-Schwartz's inequality and Parseval's theorem, PAPR of PSeIM-OTSM can be upper bounded as (7). From (7) it can be concluded that PAPR of PSeIM-OTSM is always 50%

smaller than that of OTSM, which is equal to $\frac{N(\max_{l,k} |\mathbf{X}_e[l,k]|^2)}{\sigma_s^2}$. Also, it is always equal or smaller than that of SeIM-OTSM, which is obtained as $\frac{\mu_{MB}(\max_{l,k} |\mathbf{X}_e[l,k]|^2)}{\sigma_s^2}$. Because the number of activated sequences in SeIM is always equal or larger than that of PSeIM-OTSM, i.e., $\mu_{MB} \geq \frac{N}{2}$.

PAPR

$$\begin{aligned}
& \frac{\max_{m,n} \left(\sum_{m=0}^{M-1} \sum_{n=0}^{N-1} \sum_{i=0}^{N-1} |\mathbf{X}_e[m,i]|^2 |\mathbf{W}_N[i,n]|^2 \right)}{\frac{1}{MN} \sum_{m=0}^{M-1} \sum_{n=0}^{N-1} \sum_{i=0}^{N-1} |\mathbf{X}_e[m,i]|^2 |\mathbf{W}_N[i,n]|^2} \\
& \times \frac{\max_q \left(\sum_{n=0}^{N-1} |p(qT_s - nT)|^2 \right)}{\sum_{q=0}^{NM-1} \sum_{n=0}^{N-1} |p(qT_s - nT)|^2} \\
& \leq \frac{\left(\frac{N}{2}\right)^2 \left(\max_{l,k} |\mathbf{X}_e[l,k]|^2\right) (N)}{\left(\frac{N}{2}\right) (\sigma_F^2) (N)} \\
& \leq \frac{N \left(\max_{l,k} |\mathbf{X}_e[l,k]|^2\right)}{2\sigma_F^2}. \tag{7}
\end{aligned}$$

C. The Complexity of Detection Comparison

The complexity of detection in SeIM-based systems relates to the complexity of OOK-B decoder and the complexity of the detector utilized to decode QAM-B. Accordingly, for an SeIM-OTSM frame including M delay bins and N sequency bins, MN complex additions are needed to compare the power of MN bins with the threshold in the OOK decoder [3]. In addition, the complexity of detection in OTSM when matched filter Gauss Seidel (MFGS) detector is utilized and MN sequency bins are always activated, is on the order of $O(SLMN)$ in which S denotes the number of iterations in maximal ratio combiner and L is equal or less than the number of dominant reflectors in the DSC [4]. Since in SeIM-OTSM the total number of activated sequences over each delay bin is μ_{MB} , the complexity of decoding QAM symbols in SeIM-OTSM is on the order of $O(SLM\mu_{MB})$. Hence, the total complexity is on the order of $O(MSL\mu_{MB} + MN)$. Since detecting the state of each sequency pair in PSeIM decoder is done through the comparison of sequencies power, it is implemented through $\frac{MN}{2}$ complex additions for a PSeIM frame. Since for PSeIM-OTSM only $\frac{MN}{2}$ sequencies are activated over each frame, the complexity to decode QAM symbols through the MFGS detector is on the order of $O\left(\frac{SLMN}{2} + \frac{MN}{2}\right)$. Thus, the total complexity in PSeIM-OTSM is smaller than those of OTSM and SeIM-OTSM since $\mu_{MB} \geq \frac{N}{2}$ and $SL \gg 1$.

The total complexity of detection, calculated by counting the arithmetic operations, for OTSM, SeIM-OTSM and PSeIM-OTSM are listed in Table I. It is observed that by considering $L = 9$ dominant reflectors based on the extended vehicular A (EVA) channel model and for different combinations of delay-sequency bins, we obtain around 50% and 42% improvement in complexity of detection through PSeIM-OTSM compared to OTSM and SeIM-OTSM, respectively.

TABLE I
COMPLEXITY OF DETECTION COMPARISON

M	32	32	64	128
N	32	64	64	128
S	20	29	32	37
μ_{MB}	26	52	54	110
OTSM ($SLMN$)	184320	534528	1216512	6045696
SeIM-OTSM ($SLM\mu_{MB} + MN$)	150784	436352	1030528	5211904
PSeIM-OTSM ($SLMN/2 + MN/2$)	92672	268288	609280	3031040

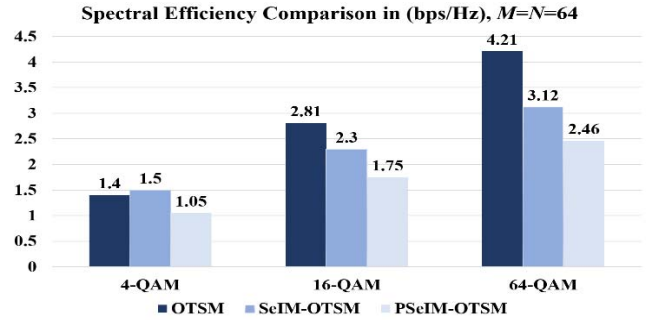


Fig. 3. SE comparison of PSeIM-OTSM, SeIM-OTSM, and OTSM.

D. The SE Comparison

In SeIM, $\mu_{MB} \log_2^Q$ bits are explicitly conveyed and N bits of OOK-B are implicitly conveyed. Hence, the SE is given as $\eta_{\text{SeIM}} = \left(1 + \frac{\mu_{MB} \log_2^Q}{N}\right)$ bps/Hz [3]. Assuming that the SE of an OTSM frame is given as $\eta_{\text{OTSM}} = \log_2^Q \left(1 - \frac{l_{\text{ZP}}}{M}\right)$ bps/Hz [3], the SE of SeIM-OTSM is $\eta_{\text{SeIM-OTSM}} = \left(1 + \frac{\mu_{MB} \log_2^Q}{N}\right) \left(1 - \frac{l_{\text{ZP}}}{M}\right)$ bps/Hz, where $l_{\text{ZP}} \geq 2l_{\text{max}} + 1$ denotes the length of ZP symbols. Since in PSeIM, $N \log_2^Q / 2$ bits are explicitly conveyed and $\frac{N}{2}$ bits are implicitly detected through OOK-B, the SE in PSeIM and PSeIM-OTSM are given as $\eta_{\text{PSeIM}} = \left(\frac{1}{2} + \frac{\log_2^Q}{2}\right)$ and $\eta_{\text{PSeIM-OTSM}} = \left(\frac{1}{2} + \frac{\log_2^Q}{2}\right) \left(1 - \frac{l_{\text{ZP}}}{M}\right)$, respectively. The SE of mentioned methods for varying Q -QAM size and different number of delay bins, sequency bins, and random number of $\frac{N}{2} \leq \mu_{MB} \leq N$ are shown in Fig. 3. In Section IV, it will be shown that, the BER trades slightly with SE in PSeIM-OTSM.

IV. PERFORMANCE EVALUATION

In this section, to assess the performance of PSeIM-OTSM, we adopt the EVA channel model with power delay profile vector of $[0, -1.5, -1.4, -3.6, -0.6, -9.1, -7, -12, -16.9]$ in dB and tap delay vector of $[0, 30, 150, 310, 370, 710, 1090, 1730, 2510]$ in ns including 9 resolvable paths with fractional delay and Doppler and independent Doppler shift at a mobility speed of 1000 kph. The MFGS detector is used at a carrier frequency of 48 GHz and bandwidth of BW=10 MHz.

In Fig. 4, the uncoded BER performance of PSeIM-OTSM is compared with SeIM-OTSM and OTSM under the same SE. As clearly seen, the analytical results obtained from (2)

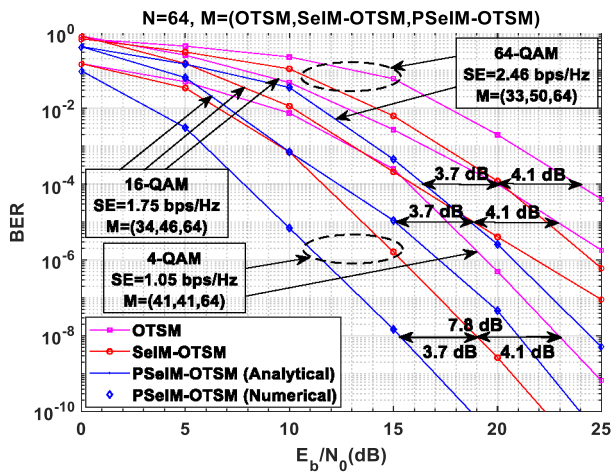


Fig. 4. The uncoded BER performance of PSeIM-OTSM, SeIM-OTSM, and OTSM for varying QAM orders in the presence of AWGN and fading.

for PSeIM-OTSM are equal to the numerical results. PSeIM-OTSM outperforms both SeIM-OTSM and OTSM for different QAM orders. For example, at a target BER of 10^{-8} , PSeIM-OTSM outclasses both SeIM-OTSM and OTSM with SNR gains of 3.7 dB and 7.8 dB, respectively, and these gains are retained for different QAM orders. As depicted in Fig. 3, the SE of PSeIM-OTSM is only 0.35, 1.05, and 1.75 bps/Hz smaller than those of OTSM where 4-QAM, 16-QAM, and 64-QAM symbols are decorated in a square DS grid of order 64, respectively. It is worth mentioning that considering the QAM orders up to 64 are practically compatible with the power requirement of green communications devices while an SNR gain of 7.8 dB at a target BER of 10^{-8} is achievable through PSeIM-OTSM with only 1.75 bps/Hz decrease in SE compared to OTSM. Therefore, according to the results in Figs. 3 and 4, the BER in PSeIM-OTSM, compared to OTSM, slightly trades with SE, which is practically acceptable.

In Fig. 5, the EE of PSeIM-OTSM is compared with those of SeIM-OTSM and OTSM under the same SE. By considering pathloss (PL) and implementation loss (IL) based on the power delay profile of EVA channel model, we evaluate the EE in bits/Joule by $EE = \frac{(SE \times BW)}{(10^{-10} \frac{SNR}{10} \times 10 \frac{PL}{10} \times 10 \frac{IL}{10})}$. Spotting a target BER of 10^{-8} , noise power of 0 dB, and IL of 3 dB, we observe that with an SE of 1.05 bps/Hz for 4-QAM transmission, the EE of PSeIM-OTSM is obtained 125.32% and 33.52% larger than those of OTSM and SeIM-OTSM, respectively. Although by increasing the QAM order the EE decreases for all schemes, the EE improvement in PSeIM-OTSM significantly increases. The cause of decrease in EE for higher QAM orders in all schemes is that the SE slightly increases; however, as depicted in Fig. 4, the 7.8 dB and 3.7 dB SNR gains, which are also obtained for higher QAM orders, are achievable at higher values of SNR, which basically leads to lower values of EE.

V. CONCLUSION

PSeIM has been introduced as a new IM technique in the DS domain to prevent bit error propagation in SeIM-based systems. The detection complexity in PSeIM-OTSM is

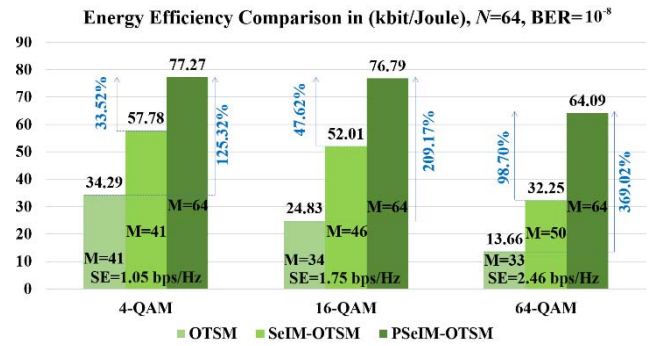


Fig. 5. EE comparison of PSeIM-OTSM, SeIM-OTSM, and OTSM.

50% and 42% lower than those of OTSM and SeIM-OTSM on average, respectively. Analytical studies and simulation results have demonstrated that the PAPR of PSeIM-OTSM is always 50% lower than that of OTSM. Also, PSeIM-OTSM outperforms both OTSM and SeIM-OTSM by 7.8 dB and 3.7 dB SNR gain, respectively. The SE in PSeIM-OTSM trades slightly with BER to avoid error propagation and take the advantages of higher EE, lower PAPR, and lower complexity of detection in PSeIM-OTSM based systems. For 4-QAM transmission and under the same SE, the EE of PSeIM-OTSM is 125.32% and 33.52% larger than those of OTSM and SeIM-OTSM, respectively. Also, this improvement of EE increases significantly by increasing the QAM order. Accordingly, PSeIM-OTSM has been proposed for green communications in vehicular wireless networks with high mobilities. Moreover, PSeIM-OTSM is a promising technique for the construction of communication systems involving in nonlinear characteristics where a low PAPR is essentially needed, such as THz and optical vehicular wireless communications.

REFERENCES

- [1] M. Saad, F. Bader, J. Palicot, A. C. A. Ghouwayel, and H. Hijazi, "Single carrier with index modulation for low power terabit systems," in *Proc. IEEE Wireless Commun. Netw. Conf. (WCNC)*, Marrakesh, Morocco, 2019, pp. 1–7.
- [2] J. Li et al., "Index modulation multiple access for 6G communications: Principles, applications, and challenges," *IEEE Netw.*, vol. 37, no. 1, pp. 52–60, Jan./Feb. 2023.
- [3] A. Doosti-Aref, E. Basar, and H. Arslan, "Sequency index modulation: A novel index modulation for delay-sequency domain waveforms," *IEEE Wireless Commun. Lett.*, vol. 12, no. 11, pp. 1911–1915, Nov. 2023.
- [4] T. Thaj and E. Viterbo, "Orthogonal time sequency multiplexing modulation," in *Proc. IEEE Wireless Commun. Netw. Conf. (WCNC)*, 2021, pp. 1–7.
- [5] T. Thaj, E. Viterbo, and Y. Hong, "Orthogonal time sequency multiplexing modulation: Analysis and low-complexity receiver design," *IEEE Trans. Wireless Commun.*, vol. 20, no. 12, pp. 7842–7855, Dec. 2021.
- [6] Y. Xin, T. Bao, J. Hua, and G. Yu, "A novel waveform scheme for THz communications," in *Proc. IEEE 94th Veh. Technol. Conf. (VTC2021-Fall)*, 2021, pp. 1–6.
- [7] T. Thaj and E. Viterbo, "Unitary-precoded single-carrier waveforms for high mobility: Detection and channel estimation," in *Proc. IEEE Wireless Commun. Netw. Conf. (WCNC)*, Austin, TX, USA, 2022, pp. 962–967.
- [8] Z. Sui, et al., "Performance analysis and approximate message passing detection of orthogonal time sequency multiplexing modulation," *IEEE Trans. Wireless Commun.*, early access, Jul. 13, 2023, doi: 10.1109/TWC.2023.3293315.
- [9] M.-S. Alouini and A. J. Goldsmith, "A unified approach for calculating error rates of linearly modulated signals over generalized fading channels," *IEEE Trans. Commun.*, vol. 47, no. 9, pp. 1324–1334, Sep. 1999.